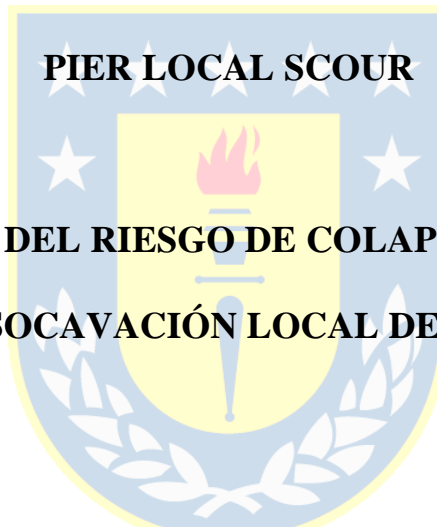




**Universidad de Concepción
Dirección de Postgrado
Facultad de Ingeniería - Programa de Magíster en Ciencias de la Ingeniería con
mención en Ingeniería Civil**

EVALUATING THE BRIDGE COLLAPSE RISK DUE TO BRIDGE



**PIER LOCAL SCOUR
(EVALUACION DEL RIESGO DE COLAPSO DE PUENTES
DEBIDO A SOCAVACIÓN LOCAL DE LAS CEPAS)**

Tesis presentada a la facultad de Ingeniería de la Universidad de
Concepción para optar al grado de Magíster en Ciencias de la Ingeniería
con Mención en Ingeniería Civil

POR CRISTIAN JOSÉ RIFO HERRERA
Profesor Guía Dr. Oscar Link Lazo

Diciembre, 2021
Concepción, Chile

Se autoriza la reproducción total o parcial, con fines académicos, por cualquier medio o procedimiento, incluyendo la cita bibliográfica del documento.



RESUMEN

A nivel mundial, los puentes fallan debido a la socavación con mayor frecuencia de lo esperado, pese a que el diseño considera escenarios desfavorables, lo que evidencia un comportamiento estocástico de la socavación y la necesidad de mejoras en los procedimientos de diseño actuales. En este trabajo, la evolución en el tiempo de la profundidad de socavación local en los pilotes de puentes se calcula mediante un modelo, considerando también el relleno de la fosa de socavación debido a la depositación de sedimentos durante la recesión de las crecidas, y se realiza un análisis de frecuencia de las series de profundidades de socavaciones máximas extremas. Los resultados obtenidos para diez puentes muestran que las series peak sobre un umbral (POT) son más adecuadas que las series de máximos anuales (AMAX) de las profundidades de socavaciones máximas, para el análisis de frecuencia. Las profundidades de las socavaciones extremas en los pilotes de puentes se distribuyen siguiendo la distribución de Cauchy. Para un período de retorno de 100 años, las profundidades de socavación en los diez puentes analizados resultaron entre un 22% y un 202% de la profundidad de socavación de equilibrio utilizada actualmente en el diseño, lo que evidencia la necesidad de un criterio diferente y más uniforme para seleccionar la profundidad de socavación de diseño. El método propuesto permite un cálculo directo de la profundidad de socavación local de diseño en función de su probabilidad de ocurrencia, lo que abre la posibilidad de introducir un diseño probabilístico para mejorar la gestión del riesgo de la infraestructura.

SUMMARY

Worldwide an important number of bridge failures due to scour occur more frequently than expected, although design considers the theoretically worst condition, evidencing a stochastic behavior of scour and the need for improvements in current design procedures. In this paper, the time evolution of local scour depth at bridge piers is computed considering refilling of the scour hole due to sediment deposition during flood recessions, and a frequency analysis of extreme maximum scour depths series is performed. Results obtained for ten bridges show that peaks over threshold (POT) series are better suited than annual-maximum (AMAX) series of maximum scour depths for frequency analysis. Extreme scour depths at bridge piers distribute following the heavy-tailed Cauchy distribution. Scour depths with a 100 years return period resulted between 22% and 202% of the equilibrium scour depth currently used in design, evidencing the need for a different, and more uniform criterion to select the design scour depth. The proposed method allows a direct computation of a design local scour depth based on its probability of occurrence, opening the possibility to introduce a probabilistic design for enhanced infrastructure risk management.

AKNOWLEDGMENTS

I want to thank Dr. Oscar Link, for his constant support and motivation during the development of this research. The Chilean Empresa de los Ferrocarriles del Estado, EFE, for providing the basic data of the railway study bridges.



INDEX OF CONTENTS

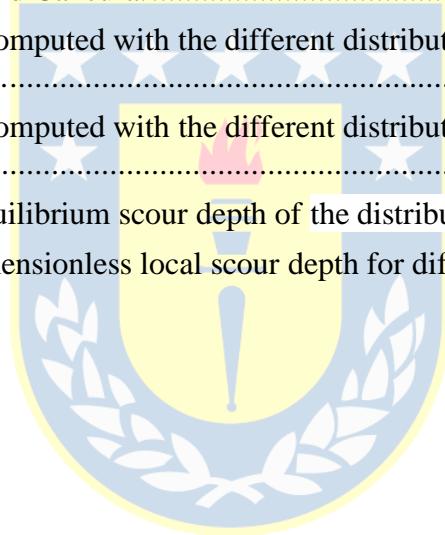
CHAPTER 1 INTRODUCTION.....	1
1.1 Motivation.....	1
1.2 Hypothesis	2
1.3 Objectives	2
1.3.1 General Objective.....	2
1.3.2 Specific Objectives.....	2
1.4 Methodology	3
1.5 Thesis Organization.....	3
CHAPTER 2 STATE OF THE ART REVIEW	4
2.1 Introduction.....	4
2.2 Probability of the scour depth.....	4
2.3 Conclusions.....	5
CHAPTER 3 MATERIALS AND METHODS	6
3.1 Introduction.....	6
3.2 Study bridges	6
3.3 Streamflow data	8
3.4 Flow velocity and flow depth computation	10
3.5 Time-dependent scour and deposition at bridge piers.....	12
3.6 Extreme scour depths series.....	15
3.7 Distribution of extreme local scour depths.....	16
3.8 Return period of equilibrium scour depth.....	18
3.9 Contribution of local scour to bridge collapse risk	18
3.10 Conclusions.....	18
CHAPTER 4 Results.....	19
4.1 Introduction.....	19
4.2 Time-dependent local scour depth at bridge piers	19
4.3 Extreme scour depths series.....	21
4.4 Extreme local scour depths distribution	21
4.5 Return period of equilibrium scour depth.....	27
4.6 Return period and risk of bridge failure due to exceedance of design local scour depth....	28
4.7 Conclusions.....	28

CHAPTER 5 GENERAL CONCLUSIONS AND COMENTARIES	30
REFERENCES	32
Appendix 4.1 GRAPHIC ANALYSIS.....	36



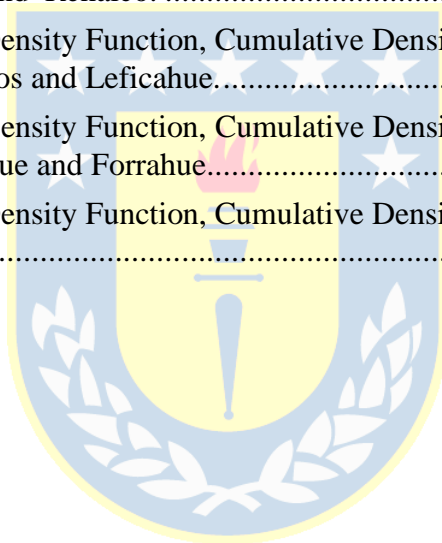
INDEX OF TABLES

Table 3.1: Main properties of the study bridges	8
Table 3.2: Streamflow gauges (SFG).....	9
Table 3.3: Parameters of the DFW model for the study bridges	15
Table 3.4: Cumulative distribution function in this study.....	17
Table 3.5: Goodness of fit statistics.....	17
Table 4.1: Efficiency for selection of series of extreme maximum scour depths	21
Table 4.2: Goodness-of-fit statistics of the distributions fitted to the POT series for Ñuble, Biobío, Renaico, Donguil and Ciruelos.	23
Table 4.3: Goodness-of-fit statistics of the distributions fitted to the POT series for Leficahue, Río Bueno, Rahue, Forrahue and Cancura.....	24
Table 4.4: Local scour depth computed with the different distributions for Ñuble, Biobío, Renaico, Donguil and Ciruelos.....	25
Table 4.5: Local scour depth computed with the different distributions for Leficahue, Río Bueno, Rahue, Forrahue and Cancura.	26
Table 4.6: Return period of equilibrium scour depth of the distribution Cauchy	27
Table 4.7: Dimension and Dimensionless local scour depth for different return periods	28



INDEX OF FIGURES

Figure 3.1: Location of study bridges.	7
Figure 3.2: Sieve curves of the riverbed sediments at the study bridges.	7
Figure 3.3: Available and missing data at the nine streamflow gauges data records.	9
Figure 3.4: Digital elevation models, Manning’s roughness coefficient and rating curves at the study bridges.	11
Figure 4.1: Computed time-dependent dimensionless local scour depth at bridges Ñuble (a), Biobío (b) Renaico (c), Donguil (d), Ciruelos (e), Leficahue (f), Bueno (g), Rahue (h), Forrahue (i), and Cancura (j). Solid line is the dimensionless equilibrium scour depth corresponding to $c1$	20
Figure A.4.1: Histogram and Density Function, Cumulative Density Function and P-P Plot of the local scour for Ñuble, Biobío and Renaico.	37
Figure A.4.2: Histogram and Density Function, Cumulative Density Function and P-P Plot of the local scour for Donguil, Ciruelos and Leficahue.	38
Figure A.4.3: Histogram and Density Function, Cumulative Density Function and P-P Plot of the local scour for Río Bueno, Rahue and Forrahue.	39
Figure A.4.4: Histogram and Density Function, Cumulative Density Function and P-P Plot of the local scour for Cancura.	40



CHAPTER 1 INTRODUCTION

1.1 Motivation

The scour depth controls the hydraulic design of a bridge, and thus the estimation of its extreme maximum value is crucial for bridge safety. In practice, design schemes are based on enveloping curves, where design scour depth is considered as that caused by an extreme flood discharge, typically associated with a return period of 100 or 200 years, which is assumed to act on the streambed during the time necessary to achieve equilibrium scour. Such design approach is adopted in e.g.: Melville and Coleman (2000), Arneson et al. (2012), MOP (2020), and DWA (2021), and leads to good safety conditions (see e.g. Shahriar et al. 2021). Even though scour-induced bridge failures occur more frequently than expected, under considerably scattered flood peak events (Wardhana and Hadipriono 2003, Cook et al. 2015, Tubaldi et al. 2017, Manfreda et al. 2018), evidencing a stochastic behaviour of scouring and the need of a different design approach.

In this work, the local scour series is determined through accurate time- dependent scour modelling, allowing a probabilistic approach for estimation of design scour depth, which would allow a more accurate bridge design and maintenance, increasing bridges safety during their service life.

1.2 Hypothesis

The contribution of local scour to the bridge collapse risk can be determined through accurate time-dependent scour modelling.

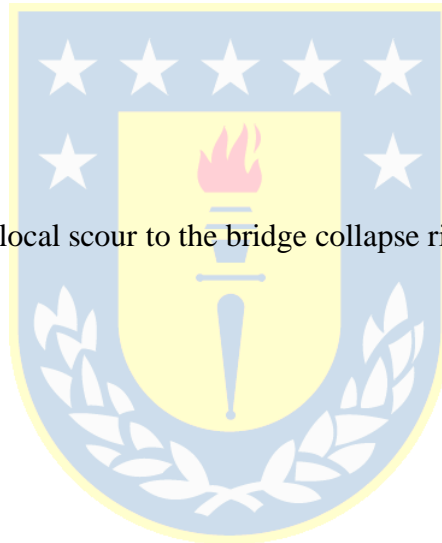
1.3 Objectives

1.3.1 General Objective

To analyze the contribution of local scour to the bridge collapse risk.

1.3.2 Specific Objectives

- a) To generate series of extreme scour depths for frequency analysis
- b) To analyze the distribution of extreme scour depths and its behavior with the return period
- c) To analyze the occurrence of extreme scour depths during the bridge service life

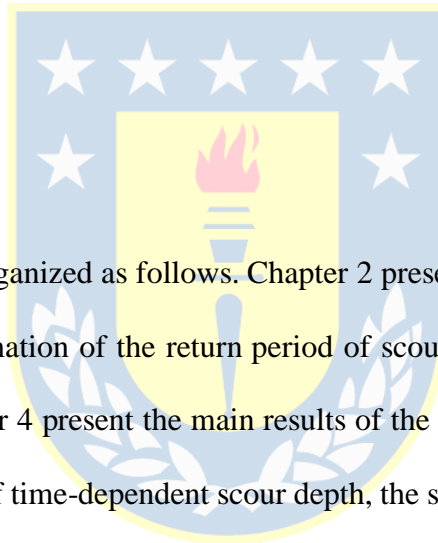


1.4 Methodology

In this work time series of scour at bridge piers are computed considering time-dependent local scour and sediment deposition. A frequency analysis of maximum scour depths considering peaks-over-threshold series (POT) and annual-maximum (AMAX) series is performed to obtain the pdf of maximum scour depths. The design scour depth is determined from a frequency analysis for a given return period corresponding to an associated risk of bridge failure.

1.5 Thesis Organization

The rest of this document is organized as follows. Chapter 2 present a review of the main theories and techniques related to estimation of the return period of scour depth. Chapter 3 describes the materials and methods. Chapter 4 present the main results of the investigation, the analysis of the study bridges, the generation of time-dependent scour depth, the selection of extreme values series and best fitting pdf, as well as the computation of return period and risk of bridge failure. Finally, in Chapter 5 is presents the analysis of obtained results and a discussion of the proposed new design philosophy and recommendations to improve bridge design, monitoring and maintenance.



CHAPTER 2 STATE OF THE ART REVIEW

2.1 Introduction

This chapter presents a brief literature review on the estimation of the probability of occurrence of extreme scour depths.

2.2 Probability of the scour depth.

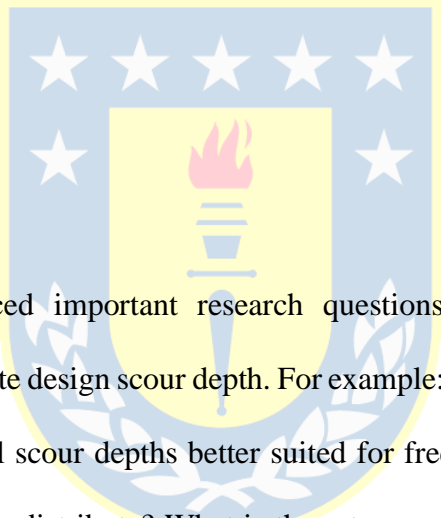
Local scour at bridge piers is an unsteady process controlled by non-linear relationships between the pier, the river sediments and the flow (Breusers et al. 1977, Raudkivi 1986, Dargahi, 1990). In particular, the complex interplay between scouring and sediment deposition produces a high variation in time of the scour depth at piers (Lu et al. 2008, Hong et al. 2016, Link et al. 2020).

Briaud et al. (2007) applied the SRICOS-EFA method by Briaud et al. (2004) to predict the scour depth versus time over the period of interest. As the SRICOS-EFA method doesn't consider sediment deposition, scour increased continuously until the end of the specified period, which is unrealistic. Hydrologic uncertainty was introduced computing final scour for thousands of equally likely hydrographs and the probability that a chosen scour depth will be exceeded was obtained from the final scour depth distribution. Manfreda et al. (2018) derived a probability distribution of scour depth, using simplified hydrographs of rectangular shape that produced a work on the scoured streambed equivalent to that produced by more realistic hydrographs. Scour depth was computed

using the model BRISENT by Pizarro et al. (2017), which similarly to the SRICOS-EFA method (Briaud et al. 2004 and 2007), doesn't consider sediment deposition, thus leading to unrealistic time histories of scour.

Recent advances in scour research allow a precise computation of the time-dependent scour depth during floods (Borghai et al. 2012, López et al. 2014, Link et al. 2017) and the effects of sediment deposition on scour, especially during the falling limb of floods (Link et al. 2020), opening the possibility of a physically based approach for accurate computation of time-dependent scour depth.

2.3 Conclusions



The literature review evidenced important research questions need to be answered for a probabilistic approach to estimate design scour depth. For example: Are annual maximum or partial duration series of extreme local scour depths better suited for frequency analysis of local scour? How does extreme scour depths distribute? What is the return period of equilibrium scour depth currently used in bridge design? What is the risk of bridge failure due to exceedance of a given design scour depth? A probabilistic approach for estimation of design scour depth would allow a more accurate bridge design and maintenance, increasing bridges safety during their service life.

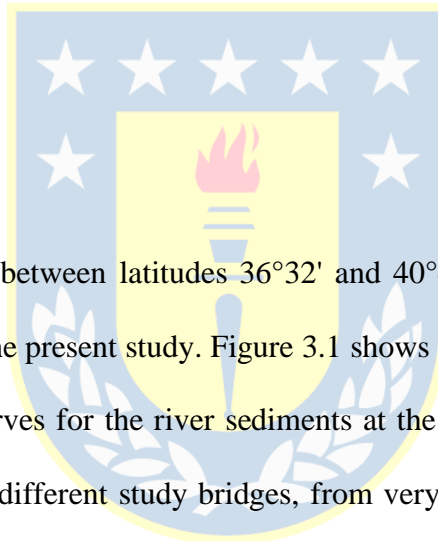
CHAPTER 3 MATERIALS AND METHODS

3.1 Introduction

In this chapter presents the materials and method for the estimation of the distribution of extreme local scour depths.

3.2 Study bridges

Ten bridges located in Chile, between latitudes $36^{\circ}32'$ and $40^{\circ}45'$ S, and longitudes $72^{\circ}5'$ and $72^{\circ}58'$ W were considered in the present study. Figure 3.1 shows the location of the study bridges. Figure 3.2 shows the sieve curves for the river sediments at the study bridges. A wide range of sediments were present at the different study bridges, from very fine sand to cobbles. Table 3.1 shows the main properties of the study bridges.



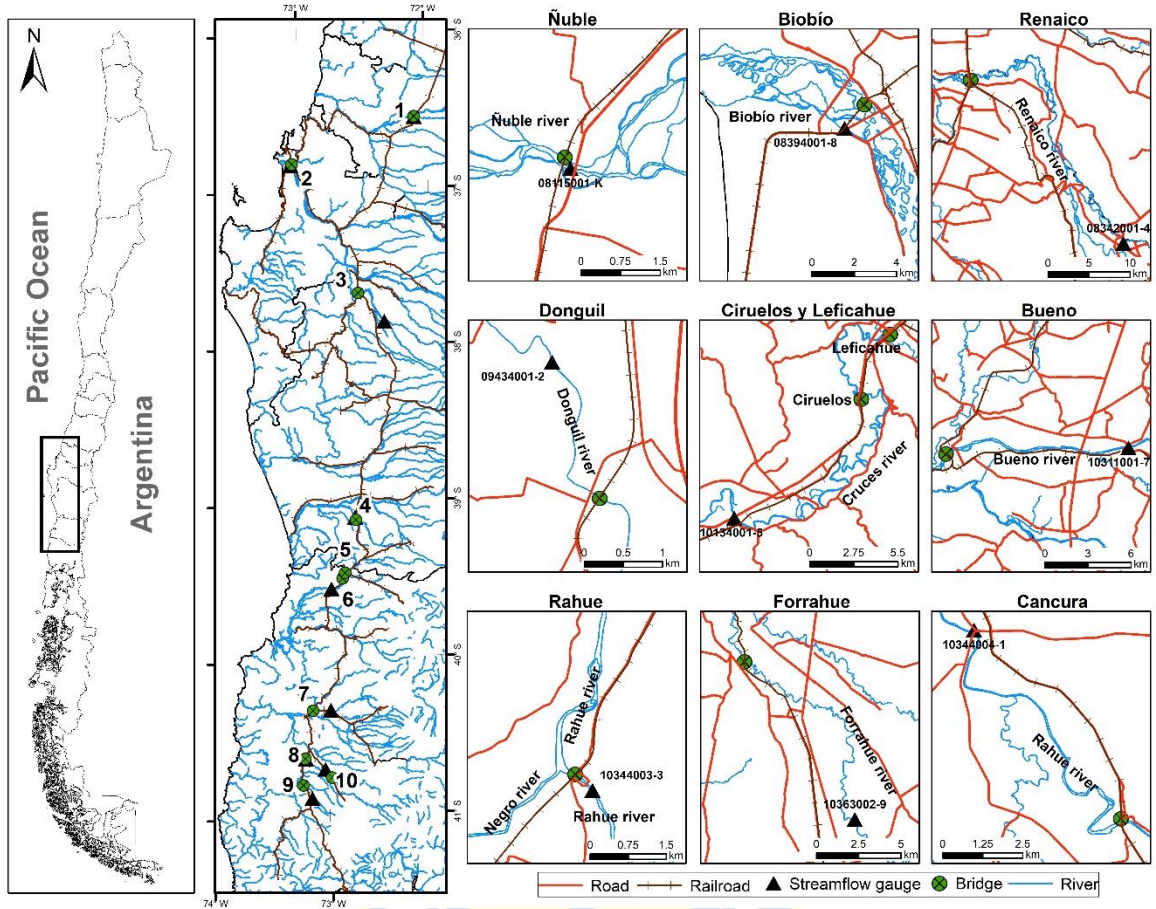


Figure 3.1: Location of study bridges.

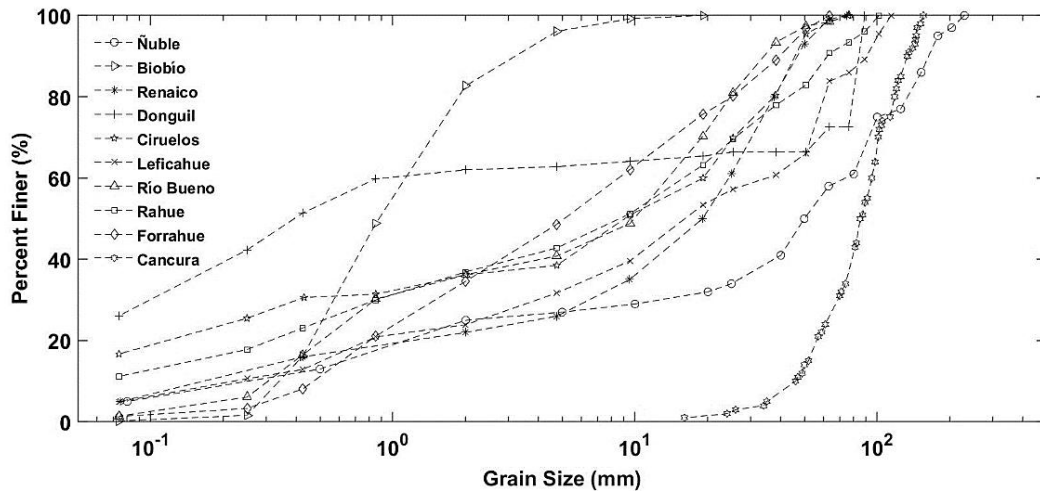


Figure 3.2: Sieve curves of the riverbed sediments at the study bridges.

Table 3.1: Main properties of the study bridges

Nr.	Bridge	Lat.	Lon.	Type	Age	Pier diameter (m)	Watershed area (km ²)	Pier Shape
1	Ñuble	36°32'S	72° 5'W	Railway	97	2.5	2,973	Cylindrical
2	Biobío	36°49'S	73° 5'W	Railway	130	0.4	21,217	Cylindrical
3	Renaico	37°40'S	72°35'W	Railway	88	4.1	1,493	Round Nose
4	Donguil	39° 7'S	72°40'W	Railway	115	2.8	739	Cylindrical
5	Ciruelos	39°29'S	72°48'W	Railway	111	2.7	1,635	Cylindrical
6	Leficahue	39°27'S	72°47'W	Railway	111	2.5	648	Cylindrical
7	Bueno	40°19'S	73° 6'W	Railway	138	2.5	4,483	Cylindrical
8	Rahue	40°37'S	73°10'W	Railway	114	2.5	2,124	Cylindrical
9	Forrahue	40°48'S	73°12'W	Railway	111	4.2	200	Rectangular
10	Cancura	40°45'S	72°58'W	Highway	43	2	1,837	Complex

3.3 Streamflow data

Time series of streamflow were obtained from the gauges (SFG) closest to the study bridges. SFG are administrated by the National Water Agency (DGA, 2021). Table 3.2 shows the available SFG for each bridge. Figure 3.3 shows the daily records for each SFG.

Flow series present different record periods and numerous information gaps of various length. To fill the gaps in the daily mean discharge series the machine learning algorithm MissForest was applied following Arriagada et al. (2021). Complete series of daily mean flows were generated for the period 1970-2016.

Table 3.2: Streamflow gauges (SFG)

ID	Bridge	SFG code	Lat.	Long.	Record Period	Altitude
1	Ñuble	8115001-K	36° 33' 00"	72° 05' 60"	1956 - 1982	107
2	Biobio	8394001-8	36° 50' 16"	73° 03' 41"	1970 - 2020	16
3	Renaico	8342001-4	37° 50' 41"	72° 23' 27"	1982 - 2019	135
4	Donguil	9434001-2	39° 07' 03"	72° 40' 44"	1947 - 2019	85
5	Ciruelos	10134001-5	39° 33' 12"	72° 54' 02"	1969 - 2020	60
6	Leficahue	10134001-5	39° 33' 12"	72° 54' 02"	1969 - 2020	60
7	Bueno	10311001-7	40° 19' 43"	72° 57' 27"	1926 - 2019	45
8	Rahue	10344003-3	40° 38' 00"	73° 10' 53"	2008 - 2020	40
9	Forrahue	10344004-1	40° 42' 21"	73° 01' 08"	2008 - 2020	50
10	Cancura	10363002-9	40° 54' 16"	73° 07' 54"	1991 - 2019	117

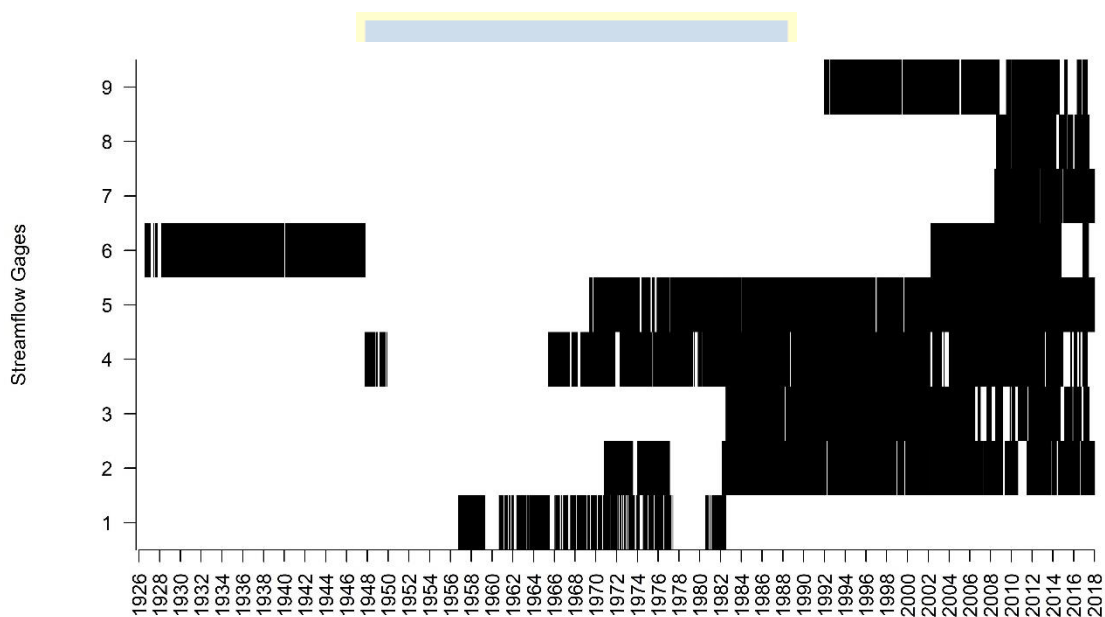


Figure 3.3: Available and missing data at the nine streamflow gauges data records.

3.4 Flow velocity and flow depth computation

Rating curves relating the flow velocity and depth with the river discharge were computed with HEC-RAS 5.0.7 software. For the simulations, digital elevation models were obtained from EFE (2020). Manning roughness coefficient was estimated through Strickler formula and Cowan method described in Chow (1994). Figure 3.4 shows the digital elevation models and rating curves for the study bridges.



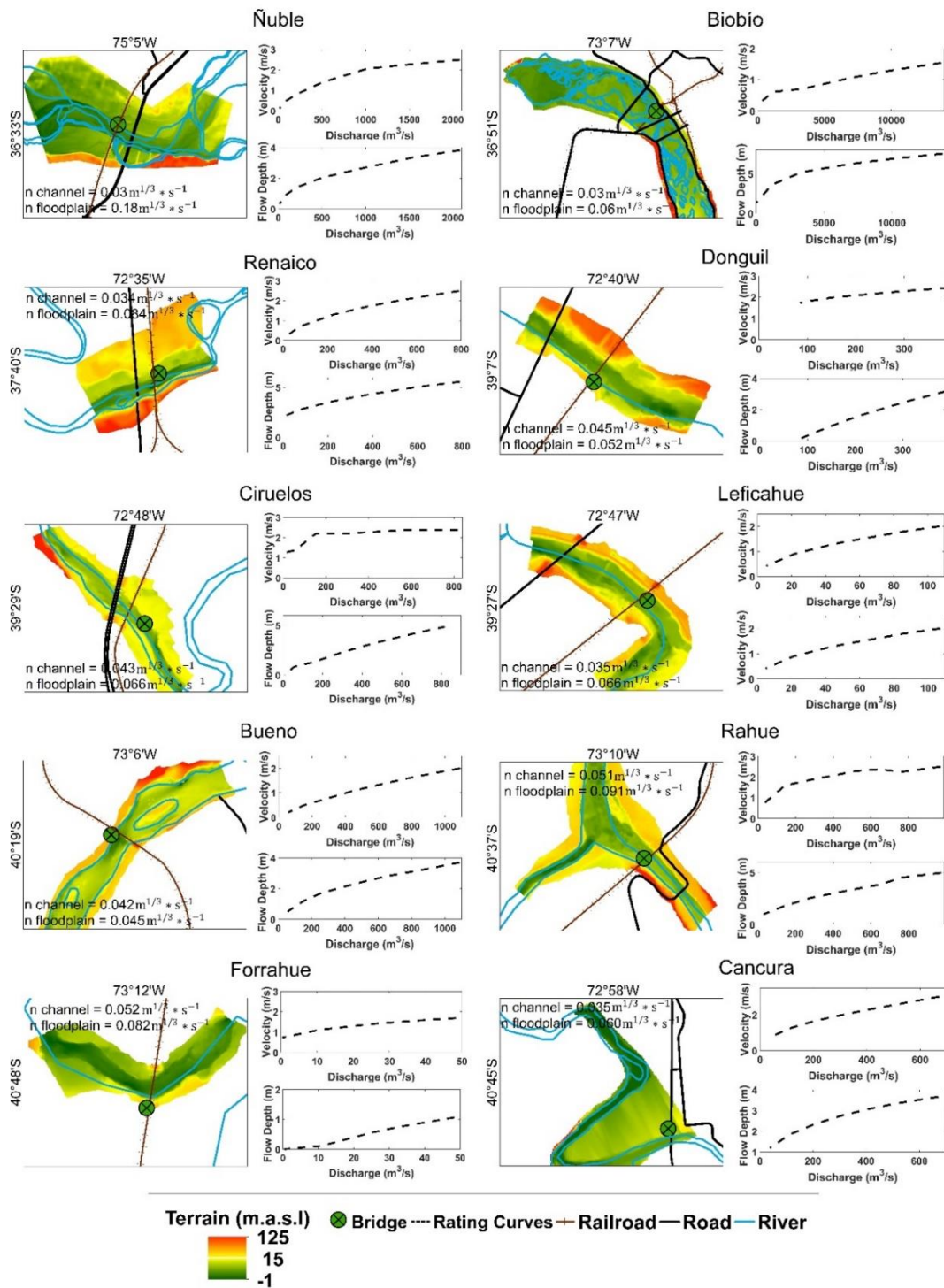


Figure 3.4: Digital elevation models, Manning's roughness coefficient and rating curves at the study bridges.

3.5 Time-dependent scour and deposition at bridge piers

The time-dependent local scour depth at bridge piers was computed with the model by Link et al. (2020). The mathematical definition of the dimensionless effective flow work W^* is:

$$W^* = \int_0^{t_{end}} \frac{Fr_d^3 u_{ef}}{z_R} \delta dt, \quad (3.1)$$

where $Fr_d = u_{ef}/\sqrt{\rho'gd_s}$ is the densimetric Froude number, $u_{ef} = u - u_{cs}$ is the excess velocity above the incipient scour condition $u_{cs} (= 0.5u_c)$, u is the average flow velocity, u_c is the critical velocity for the inception of sediment motion at the undisturbed bed, $z_R = D^2/2d_s$ is a reference length, D is the pier diameter, d_s is the representative sediment particle diameter (e.g., d_{50}), t_{end} is a considered time for analysis purposes (e.g., hydrograph duration for event-scale analysis), and δ is the delta Dirac function,

$$\delta = \begin{cases} 0 & u/u_{cs} < 1.0 \\ 1 & u/u_{cs} \geq 1.0 \end{cases} \quad (3.2)$$

The DFW model uses a three-parameter exponential relationship between W^* and the normalised scour depth $Z^* (= z_s/z_R)$ which is reported in Eq. (3.3):

$$Z^* = c_1(1 - \exp(-c_2W^{c_3})), \quad (3.3)$$

where z_s is the dimensional scour depth, whereas c_1 , c_2 , and c_3 are model coefficients. It is worthy to note that c_1 corresponds to the equilibrium scour depth:

$$c_1 = Z_{eq}^* = z_{eq} \left(\frac{2d_s}{D^2} \right), \quad (3.4)$$

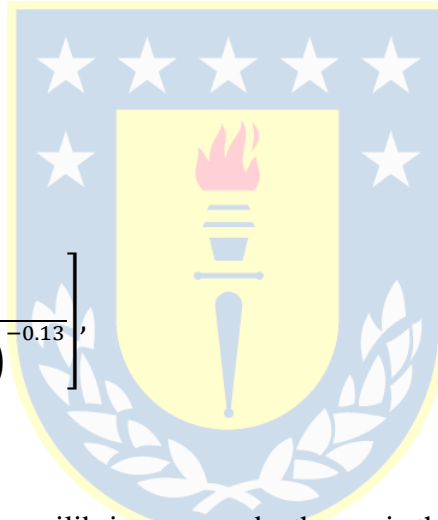
The equilibrium scour depth was computed with the scour formula by Sheppard *et al.* (2014):

$$\frac{z_{eq}}{a^*} = 2.5f_1f_2f_3, \quad 0.4 \leq \frac{u}{u_c} < 1.0 \quad (3.5)$$

$$f_1 = \tanh \left[\left(\frac{h}{a^*} \right)^{0.4} \right], \quad (3.6)$$

$$f_2 = \left\{ 1 - 1.2 \left[\ln \left(\frac{u}{u_c} \right) \right]^2 \right\}, \quad (3.7)$$

$$f_3 = \left[\frac{\left(\frac{a^*}{d_s} \right)}{0.4 \left(\frac{a^*}{d_s} \right)^{1.2} + 10.6 \left(\frac{a^*}{d_s} \right)^{-0.13}} \right], \quad (3.8)$$



where Z_{eq}^* is the dimensionless equilibrium scour depth, z_{eq} is the dimensional equilibrium scour depth, a^* ($= K_s a_p$) is the effective diameter of the pier, K_s is the shape factor, a_p is the projected width of the pier, h is the flow depth. Besides, u_c was computed following Zanke's equation (Zanke 1977):

$$u_c = 1.4(\sqrt{\rho'gd_s} + 10.5\nu/d_s), \quad (3.9)$$

On the other side, c_2 and c_3 can take values according to geometrical, flow, and sediment properties. Sediment deposition refers herein to the refilling process of the scour hole. Deposition occurs when the sediment supply rate of sediment particles into the scour hole is greater than the local sediment transport capacity:

$$z_{d[i]} = \begin{cases} 0, & \xi g_{s[i-1,j]}^* \leq g_{s[i,j]}^* \\ \frac{\alpha}{\rho_s(1-p)} \sum_{j=1}^n \left(\frac{\xi g_{s[i-1,j]}^* - g_{s[i,j]}^*}{z_{i-1}} \right) \Delta t, & \xi g_{s[i-1,j]}^* > g_{s[i,j]}^* \end{cases} \quad (3.10)$$

where $z_{d[i]}$ is the sediment deposition depth, j is a counter for the considered sediment sizes in the sieve curve and i reports the discrete-time instant, p is the riverbed porosity, g_s^* is the sediment transport capacity, ξg_s^* is the sediment supply rate, and α and ξ are calibration parameters. It is worthy to note that ξ is an exceedance sediment supply coefficient, whereas the final scour depth – considering both the erosive and refilling processes – at each temporal instant i , was computed as $z_{[i]} = z_{s[i]} - z_{d[i]}$ and $W_{[i]}^* = W_{s[i]}^* - \Delta W_{d[i]}^*$ (note that the subscripts “s” and “d” are used for scour and deposition, respectively). Finally, g_s^* was estimated using Meyer-Peter and Müller equation (Meyer-Peter and Müller 1948):

$$g_s^* = 8\rho_s(\rho'gd_s^3)^{0.5} \left[\left(\frac{C_R}{C'_R} \right)^{1.5} \theta - \theta_c \right]^{1.5} \quad (3.11)$$

where C_R is the total Chézy coefficient due to effective bed roughness k_s ($= 18 \log \log (12h/k_s)$), C'_R is the Chézy coefficient due to particle roughness d_{90} ($= 18 \log \log (12h/d_{90})$), and θ and θ_c are the Shields and threshold Shields parameters. Table 3.3

shows the parameters for computation of time-dependent pier scour depth with the DFW model at the study bridges.

Table 3.3: Parameters of the DFW model for the study bridges

	ξ	α	c_1	c_2	c_3	$D_{50}(mm)$	$D_{90}(mm)$	$D(m)$	S
Ñuble	4.0	0.00020	0.0800	0.031	0.23	50.0	163.6	2.5	0.0020
Biobío	2.5	0.00020	0.0100	0.010	0.37	0.92	3.200	0.3	0.0002
Renaico	2.5	0.00020	0.0120	0.040	0.27	20.0	47.49	4.1	0.0029
Donguil	2.5	0.00200	0.0003	0.010	0.30	0.40	84.26	2.5	0.0010
Ciruelos	2.5	0.02250	0.0250	0.028	0.25	8.69	45.86	2.7	0.0020
Leficahue	2.5	0.00020	0.0060	0.028	0.30	8.84	62.36	2.5	0.0025
Bueno	2.5	0.00002	0.0150	0.030	0.30	10.1	34.60	2.5	0.0070
Rahue	2.5	0.00020	0.0350	0.031	0.23	24.8	81.95	2.5	0.0010
Forrahue	2.5	0.00225	0.0015	0.028	0.28	5.25	39.75	4.2	0.0060
Cancura	5.0	$1 * 10^{-9}$	0.1800	0.010	0.20	85.0	133.0	2.0	0.0740

3.6 Extreme scour depths series

A main issue to be tackled for the frequency analysis of extreme maximum scour depths is the selection of values to build the time series of extreme values. Following Cunnane (1973), two time series commonly used in floods frequency analysis were evaluated, namely peaks-over-threshold (POT) and maximum annual series (AMAX). For a POT series a threshold value was established for the choice of the magnitudes of the local scour (a value per year that exceeds the limit value) following the methodology proposed by Lang *et al.* (1999). As a general rule, a minimum of 30 data was established on the threshold value for the frequency analysis of the local scour. The best series for frequency analysis was selected according to the efficiency:

$$E = \frac{\text{var}(Z_s(T)_{AMAX})}{\text{var}(Z_s(T)_{POT})} \quad (3.12)$$

where E is efficiency, var is the variance, $Z_s(T)$ is the local scour depth corresponding to a return period of T years. Efficiencies $E > 1$ suggest POT series is better, $E < 1$ suggest that AMAX series is better, and $E = 1$ suggest that both series are equally good for frequency analysis.

3.7 Distribution of extreme local scour depths

The maximum likelihood method was applied to fit probability distributions representing the series of extreme maximum scour depths. Table 3.4 shows the cumulative probability distribution functions for analysis.

The goodness-of-fit was determined for each probability distribution through the test Kolmogorov-Smirnov (KS), χ^2 , Anderson-Darling (AD) with a significance level of 0.05, a graphic analysis, and the coefficient of determination (r^2), as shown in Table 3.5.

Where n is the simple size, $F(x)$ is the theoretical cumulative distribution function, $F_n(x)$ is the empirical cumulative distribution function, k is the class intervals, O_i is the observed absolute frequency and E_i is the theoretical frequency in interval i , $\sup ||$ is the largest absolute difference, \hat{y}_i is the fitted value, \bar{y} is the mean, and y_i is the observed values of the dependent variable.

Table 3.4: Cumulative distribution function in this study

Distribution	Cumulative Distribution Function	Parameter
Normal	$F(x) = (\sqrt{2\pi})^{-1} \int_0^z e^{-t^2/2} dt \left(\frac{x-\mu}{\sigma} \right)$	μ : Location parameter σ : Scale parameter
Lognormal	$F(x) = (\sqrt{2\pi})^{-1} \int_0^z e^{-t^2/2} dt \left(\frac{\ln(x-\gamma)-\mu}{\sigma} \right)$	γ : Location parameter μ : Scale parameter σ : Shape parameter
Weibull	$F(x) = 1 - \exp \left[- \left(\frac{x-\gamma}{\beta} \right)^\alpha \right]$	γ : Location parameter β : Scale parameter α : Shape parameter
Gamma	$F(x) = \frac{\Gamma_{((x-\gamma)/\beta)}(\alpha)}{\Gamma(\alpha)}$ Γ_z : Incomplete gamma function	γ : Location parameter β : Scale parameter α : Shape parameter
Gumbel	$F(x) = \frac{1}{\beta} \exp \left[- \frac{x-\mu}{\beta} - e^{-\frac{x-\mu}{\beta}} \right]$	μ : Location parameter β : Scale parameter
Cauchy	$F(x) = \frac{1}{2} + \frac{1}{\pi} \tan^{-1} \left(\frac{x-\mu}{\sigma} \right)$	μ : Location parameter σ : Scale parameter

Table 3.5: Goodness of fit statistics

Statistics	General Formula
r^2	$\frac{\sum_{i=1}^n (\hat{y}_i - \bar{y})^2}{\sum_{i=1}^n (y_i - \bar{y})^2}$
KS	$\sup F_n(x) - F(x) $
χ^2	$\sum_{i=1}^k \frac{(O_i - E_i)^2}{E_i}$
AD	$n \int_{-\infty}^{\infty} \frac{[F_n(x) - F(x)]^2}{F(x)[1 - F(x)]} dF(x)$

3.8 Return period of equilibrium scour depth

The return period of a given scour depth was determined from the selected probability distribution function, as the inverse of the exceedance probability.

3.9 Contribution of local scour to bridge collapse risk

The contribution of local scour to bridge collapse risk was computed through the hydrological risk R that a flood with a return period equal to T is exceeded during the design life, L_t , of the bridge:

$$R = 1 - (1 - 1/T)^{L_t} \quad (3.13)$$

In the present study, a service life of 60 years was adopted for the study bridges.

3.10 Conclusions

In this chapter, the methods for the estimation of the distribution of extreme local scour depths, for 10 bridges in Chile were presented. The proposed method allows a direct computation of design local scour depth at bridge piers based on its probability of occurrence, opening the possibility to introduce a probabilistic design for enhanced infrastructure risk management.

CHAPTER 4 Results

4.1 Introduction

In this chapter, the principal results of the investigation are presented. First, time-dependent local scour depth at bridge piers. The efficiency for selection of series of extreme maximum scour depths at study bridges. The goodness-of-fit statistics of the distributions and the computed local scour depth for different return periods and risk at the study bridges.

4.2 Time-dependent local scour depth at bridge piers

Figure 4.1 shows the computed time-dependent local scour depth for the studies bridges according to parameters in Table 3.3.

The resulting scour is highly dynamic in time, with important variations during the study period (1970-2016). Seven out of ten cases (a, b, c, e, g, I and j) presented sediment deposition that was able to reverse scour to zero several times, while cases d, f and h presented scour depth higher than zero during the whole period. In all cases, the number of local maxima was higher than the number of years under analysis. Noteworthy, some sites exhibited similar scour maxima (e.g.: cases a, e, h and j) while others exhibited maxima with notable different magnitudes (e.g.: cases b and g).

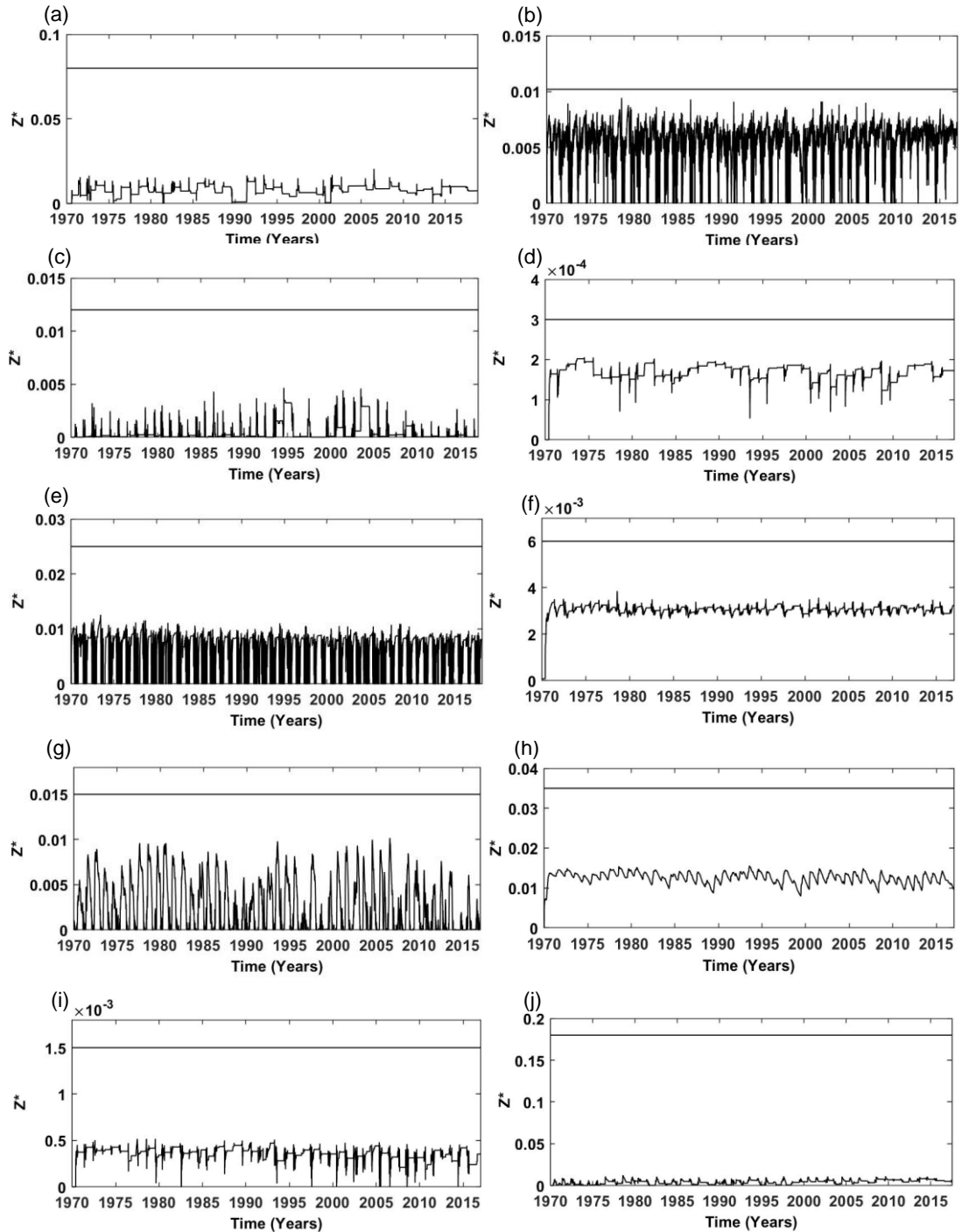


Figure 4.1: Computed time-dependent dimensionless local scour depth at bridges Ñuble (a), Biobío (b), Renaico (c), Donguil (d), Ciruelos (e), Leficahue (f), Bueno (g), Rahue (h), Forrahue (i), and Cancura (j). Solid line is the dimensionless equilibrium scour depth corresponding to c_1 .

4.3 Extreme scour depths series

Table 4.1 shows the efficiency for selection of series of extreme maximum scour depths at study bridges for different return periods.

Efficiency, $E > 1$, in 24 out of 40 cases; $E = 1$ in 7 cases, and $E < 1$ in 9 cases. Consequently, the POT series were in general equal or better ($24+7 = 31$ out 40) than the AMAX series for frequency analysis of maximum local scour depths, and are thus selected for the frequency analysis.

Table 4.1: Efficiency for selection of series of extreme maximum scour depths

T	Ñuble	Biobío	Renaico	Donguil	Ciruelos	Leficahue	Bueno	Rahue	Forrahue	Cancura
25	1.19	1.22	0.94	1.0	0.73	1.04	0.91	1.00	1.16	1.22
50	1.22	1.22	0.94	1.0	0.74	1.04	1.00	1.01	1.16	1.23
100	1.26	1.22	0.93	1.0	0.75	1.04	1.00	1.02	1.16	1.24
200	1.29	1.22	0.93	1.0	0.76	1.03	1.03	1.03	1.17	1.25

4.4 Extreme local scour depths distribution

Table 4.2 and 4.3 shows the goodness-of-fit statistics of the distributions fitted to the POT series for the study bridges. Graphics with the probability density, histogram, cumulative distribution and P-P plots are included in the appendix 4.1.

All candidate pdfs presented acceptable goodness-of-fit statistics. Further, Table 4.4 and 4.5 shows the local scour depth computed with the different distributions.

Scour depths computed with Weibull, Normal, Lognormal, Gamma and Gumbel distributions presented a very low or no sensitivity with the return period, which is not realistic. Instead, the Cauchy distribution computed realistic variations of scour magnitudes with the return period. Thus, it was selected as the best distribution representing extreme local scour depths at bridges.



Table 4.2: Goodness-of-fit statistics of the distributions fitted to the POT series for Ñuble, Biobío, Renaico, Donguil and Ciruelos.

Bridge	Distribution	Goodness-of-fit statistic			
		K-S	χ^2	A-D	r^2
Ñuble	Cauchy	0.15	1.61	1.17	0.66
	Weibull	0.11	0.83	0.57	0.95
	Normal	0.14	6.45	0.62	0.97
	Lognormal	0.16	3.82	0.66	0.96
	Gamma	0.16	5.44	0.64	0.97
	Gumbel	0.17	3.83	0.73	0.93
Biobío	Cauchy	0.19	3.91	1.99	0.67
	Weibull	0.17	2.89	1.73	0.83
	Normal	0.17	3.14	1.13	0.92
	Lognormal	0.16	3.36	1.01	0.94
	Gamma	0.16	3.19	1.05	0.93
	Gumbel	0.12	0.55	0.54	0.98
Renaico	Cauchy	0.16	1.1	1.08	0.64
	Weibull	0.13	3.66	0.57	0.97
	Normal	0.14	2.9	0.65	0.96
	Lognormal	0.13	4.41	0.75	0.97
	Gamma	0.14	5.32	0.66	0.97
	Gumbel	0.13	7.38	0.77	0.96
Donguil	Cauchy	0.16	1.72	1	0.71
	Weibull	0.14	1.84	1.01	0.88
	Normal	0.12	1.98	0.56	0.96
	Lognormal	0.12	2.3	0.51	0.96
	Gamma	0.12	2.06	0.53	0.96
	Gumbel	0.11	1.96	0.37	0.98
Ciruelos	Cauchy	0.14	0.19	0.55	0.8
	Weibull	0.18	2.75	1.56	0.82
	Normal	0.14	1.09	0.58	0.91
	Lognormal	0.13	1.6	0.46	0.93
	Gamma	0.13	0.85	0.49	0.92
	Gumbel	0.09	0.04	0.23	0.97

Table 4.3: Goodness-of-fit statistics of the distributions fitted to the POT series for Leficahue, Río Bueno, Rahue, Forrahue and Cancura.

Bridge	Distribution	Goodness-of-fit statistic			
		K-S	χ^2	A-D	r^2
Leficahue	Cauchy	0.15	3.09	1.05	0.78
	Weibull	0.23	3.61	3.02	0.72
	Normal	0.14	1.86	1.05	0.82
	Lognormal	0.13	1.81	0.93	0.83
	Gamma	0.14	1.48	0.97	0.83
	Gumbel	0.12	0.43	0.43	0.91
Río Bueno	Cauchy	0.12	0.44	0.68	0.73
	Weibull	0.08	2.18	0.23	0.99
	Normal	0.1	2.61	0.34	0.98
	Lognormal	0.13	3.97	0.53	0.96
	Gamma	0.12	4.06	0.45	0.97
	Gumbel	0.16	5.84	0.84	0.91
Rahue	Cauchy	0.12	6.61	1.1	0.79
	Weibull	0.09	0.84	0.47	0.97
	Normal	0.1	4.02	0.31	0.98
	Lognormal	0.11	5.15	0.36	0.98
	Gamma	0.1	3.46	0.34	0.98
	Gumbel	0.13	7.33	0.85	0.94
Forrahue	Cauchy	0.19	1.95	1.65	0.65
	Weibull	0.19	2.81	1.87	0.81
	Normal	0.17	2.47	1.34	0.9
	Lognormal	0.17	2.62	1.22	0.91
	Gamma	0.17	2.52	1.26	0.91
	Gumbel	0.13	1.65	0.7	0.95
Cancura	Cauchy	0.17	3.34	1.47	0.67
	Weibull	0.14	4.35	0.96	0.9
	Normal	0.15	5.15	1.05	0.94
	Lognormal	0.14	5.66	1.06	0.94
	Gamma	0.15	5.35	1.06	0.94
	Gumbel	0.15	12.88	1.11	0.93

Table 4.4: Local scour depth computed with the different distributions for Ñuble, Biobío, Renaico, Donguil and Ciruelos.

Bridge	Distribution	$Z_s(m)$			
		T=25	T=50	T=100	T=200
Ñuble	Cauchy	1.6	2.4	4	7.11
	Weibull	1.05	1.08	1.1	1.12
	Normal	1.07	1.11	1.14	1.17
	Lognormal	1.09	1.14	1.19	1.24
	Gamma	1.08	1.13	1.17	1.21
	Gumbel	1.15	1.22	1.3	1.38
	Biobío	Cauchy	0.5	0.6	0.79
Weibull		0.46	0.46	0.47	0.47
Normal		0.46	0.46	0.47	0.47
Lognormal		0.46	0.46	0.47	0.48
Gamma		0.46	0.46	0.47	0.48
Gumbel		0.46	0.47	0.48	0.49
Renaico		Cauchy	3.34	5.56	9.98
	Weibull	1.86	1.97	2.07	2.16
	Normal	1.85	1.96	2.07	2.17
	Lognormal	2.01	2.23	2.44	2.66
	Gamma	1.93	2.1	2.26	2.42
	Gumbel	2.02	2.25	2.48	2.7
	Donguil	Cauchy	1.78	2.09	2.77
Weibull		1.58	1.6	1.61	1.62
Normal		1.58	1.6	1.62	1.63
Lognormal		1.59	1.6	1.62	1.64
Gamma		1.59	1.6	1.62	1.64
Gumbel		1.61	1.64	1.67	1.7
Ciruelos		Cauchy	5.47	6.53	8.67
	Weibull	4.96	5.02	5.08	5.13
	Normal	4.9	4.98	5.05	5.12
	Lognormal	4.91	4.99	5.07	5.14
	Gamma	4.91	4.99	5.06	5.13
	Gumbel	4.96	5.1	5.23	5.37

Table 4.5: Local scour depth computed with the different distributions for Leficahue, Río Bueno, Rahue, Forrahue and Cancura.

Bridge	Distribution	$Z_s(m)$			
		T=25	T=50	T=100	T=200
Leficahue	Cauchy	1.36	1.53	1.86	2.53
	Weibull	1.29	1.3	1.31	1.32
	Normal	1.27	1.28	1.29	1.3
	Lognormal	1.27	1.28	1.3	1.31
	Gamma	1.27	1.28	1.3	1.31
	Gumbel	1.27	1.29	1.31	1.33
Río Bueno	Cauchy	4.28	5.98	9.37	16.14
	Weibull	3.09	3.16	3.22	3.27
	Normal	3.16	3.26	3.36	3.44
	Lognormal	3.23	3.37	3.51	3.63
	Gamma	3.2	3.33	3.45	3.56
	Gumbel	3.47	3.72	3.96	4.2
Rahue	Cauchy	1.99	2.42	3.3	5.01
	Weibull	1.69	1.71	1.72	1.74
	Normal	1.7	1.73	1.75	1.77
	Lognormal	1.71	1.74	1.76	1.79
	Gamma	1.7	1.73	1.76	1.78
	Gumbel	1.78	1.84	1.9	1.96
Forrahue	Cauchy	0.94	1.1	1.4	2.08
	Weibull	0.86	0.87	0.88	0.88
	Normal	0.86	0.87	0.88	0.89
	Lognormal	0.86	0.87	0.88	0.9
	Gamma	0.86	0.87	0.88	0.89
	Gumbel	0.86	0.88	0.9	0.92
Cancura	Cauchy	0.4	0.57	0.9	1.62
	Weibull	0.27	0.28	0.28	0.29
	Normal	0.27	0.28	0.29	0.29
	Lognormal	0.27	0.28	0.29	0.3
	Gamma	0.27	0.28	0.29	0.3
	Gumbel	0.28	0.3	0.32	0.33

4.5 Return period of equilibrium scour depth

Table 4.6 shows the equilibrium scour and corresponding return period computed from the Cauchy probability distribution function.

The return period of the equilibrium local scour was higher than 100 years in 6 out of ten study bridges, and less than 100 years in 4 of the study bridges. It presented important variability among the study bridges, ranging between 25 and 570 years, which evidences the lack of a consistent criteria for determination of design scour depth in current design methods. Conversely, scour depth with a 100 years return period resulted between 22% and 202% of the equilibrium scour depth currently used in design.

Table 4.6: Return period of equilibrium scour depth of the distribution Cauchy

Study site	Z_{eq} (m)	Z_{eq}^*	T (years)
Ñuble	5.0	0.0800	133
Biobío	0.5	0.0100	25
Renaico	5.0	0.0120	43
Donguil	2.3	0.0003	65
Ciruelos	10.5	0.0250	140
Leficahue	2.1	0.0060	133
Río Bueno	4.6	0.0150	30
Rahue	4.4	0.0350	168
Forrahue	2.5	0.0015	270
Cancura	4.2	0.1800	570

4.6 Return period and risk of bridge failure due to exceedance of design local scour depth

Table 4.7 shows the computed local scour depth for different return periods and risk at the study bridges.

The magnitude of local scour depth at bridge piers corresponding to a given return period present a high variation among the study sites.

Table 4.7: Dimension and Dimensionless local scour depth for different return periods

Bridge	<i>T</i> 25 (years)		<i>T</i> 50 (years)		<i>T</i> 100 (years)		<i>T</i> 200 (years)	
	<i>R</i> = 90%		<i>R</i> = 70%		<i>R</i> = 50%		<i>R</i> = 26%	
	$Z_s(m)$	Z^*	$Z_s(m)$	Z^*	$Z_s(m)$	Z^*	$Z_s(m)$	Z^*
Ñuble	1.63	0.0261	2.41	0.0386	3.98	0.0637	7.11	0.1138
Biobío	0.50	0.0103	0.60	0.0123	0.79	0.0162	1.17	0.0240
Renaico	3.34	0.0079	5.56	0.0132	9.98	0.0237	18.82	0.0448
Donguil	1.78	0.0002	2.09	0.0003	2.77	0.0004	3.99	0.0005
Ciruelos	5.47	0.0130	6.53	0.0156	8.67	0.0207	12.93	0.0308
Leficahue	1.36	0.0038	1.53	0.0043	1.86	0.0053	2.53	0.0072
Río Bueno	4.28	0.0138	5.98	0.0193	9.37	0.0303	16.14	0.0522
Rahue	1.99	0.0158	2.42	0.0192	3.28	0.0261	5.01	0.0397
Forrahue	0.94	0.0006	1.10	0.0007	1.42	0.0008	2.08	0.0012
Cancura	0.40	0.0168	0.57	0.0243	0.92	0.0392	1.62	0.0689

4.7 Conclusions

In this chapter, the time dependence of the local scour was calculated, obtaining that the partial duration series considering peaks over a threshold (POT) is more efficient for the frequency

analysis. Through goodness of fit tests with a significance level of 0.05 and graphical analysis the extreme scour depths at bridge piers distributed following a Cauchy distribution.

Scour depths with a 100 years return period resulted between 22% and 202% of the equilibrium scour depth currently used in design.

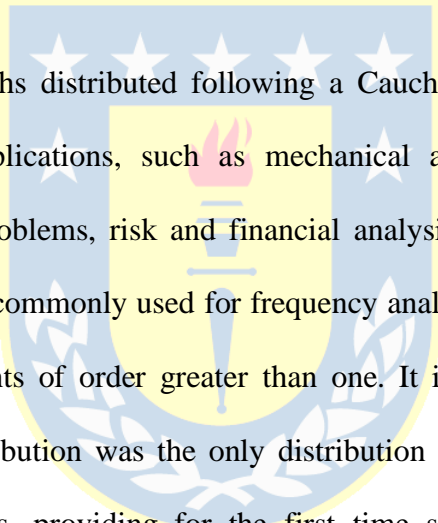


CHAPTER 5 CONCLUSIONS

Current standards in hydraulic bridge design consider a design scour depth which corresponds to the equilibrium scour. In practice, equilibrium scour is computed for a worst case scenario given by an extreme flood, assuming that its duration is longer than that needed to develop and achieve equilibrium scour. An important shortcoming of such design approach is that magnitudes of resulting design scour are not associated to an exceedance probability nor to a return period. Consequently, risk of failure due to scour can't be computed. Probabilistic scour estimations were proposed in the past through uncertainty analysis (e.g.: Johnson 1992, Johnson and Dock 1998, Bolduc et al. 2008), where the developed probabilistic models for the final scour depth were used to assess the probability that a specified threshold depth is exceeded at a bridge pier for given hydrologic variables considering model, hydraulic, and/or parameter uncertainties. In this work, a different approach was followed.

Obtained time-dependent scour (Fig. 4.1) was very sensible to the involved case-specific model parameters (Table 3.3), presenting noticeable differences among the study bridges. The scour-deposition model adequately differentiated between the study cases and produced realistic scour. Alternative methods for the time-dependent scour, such as those by Zanke (1982) or Dey (1999), could also be applied. In the proposed method, constant c_1 was evaluated with the scour formula by Sheppard et al. (2014), which is conservative as it neglects the possible effects of armoring. Different scour formulas could be used as an alternative to Sheppard et al. (2014) for estimation of c_1 , such as those proposed by Jain and Fischer (1979 and 1980) for bridges in supercritical flows, or Qi et al. (2016) for Chinese rivers.

The resulting time-dependent scour presented important variations during the study period. In some cases, scour maxima were similar while in others cases, they exhibited maxima with notable different magnitudes. Series of extreme scour depths were computed with the annual maxima (AMAX) and partial duration series considering peaks over a threshold (POT). According to the efficiency, POT series exhibited smaller variances of local scour depth corresponding to a return period of T years than AMAX series, and thus, POT was preferred for frequency analysis. Similarly to the flood frequency analysis, the use of both type of series for scour analysis present advantages and disadvantages as analyzed by Zadeh et al. (2019).



Extreme maximum scour depths distributed following a Cauchy distribution, which has been previously used in many applications, such as mechanical and electrical theory, physical anthropology, measurement problems, risk and financial analysis (Alzaatreh et al. 2016). It is different to other distributions commonly used for frequency analysis of extreme values, because it does not have finite moments of order greater than one. It is recognized as a heavy-tailed distribution. The Cauchy distribution was the only distribution able to compute realistic scour depths for high return periods, providing for the first time scour estimations associated to exceedance probabilities obtained from frequency analysis of extreme values.

The proposed methodology for estimation of local scour depth at piers can be easily applied for other scour processes involved in bridge design, such as the general scour, contraction scour, and abutment scour. The involved new design philosophy considers scour as a stochastic process, and design scour is determined for a given return period. In this way, bridge design can be associated with probability of occurrence, and risk. At the same time, the method can be applied to inform monitoring and maintenance, improving bridges safety.

REFERENCES

Alzaatreh, A., Lee, C., Famoye, F., and Ghosh, I. (2016). The generalized Cauchy family of distributions with applications. **Journal of Statistical Distributions and Applications**, **3(1)**.12.

Arneson, L.A., Zevenbergen, L.W., Lagasse, P.F., Clopper, P.E. (2012). **Evaluating Scour at Bridges. Hydraulic Engineering Circular No. 18, 5th ed.** FHWA-HIF-12-003; U.S. DOT: Washington, DC, USA (2012).340.

Arriagada, P., Karelovic, B., and Link, O. (2021). Automatic gap-filling of daily streamflow time series in data-scarce regions using a machine learning algorithm. **Journal of Hydrology**, **598(2021)**. 126454.

Bolduc, L. C., Gardoni, P., and Briaud, J. (2008). Probability of Exceedance Estimates for Scour Depth around Bridge Piers. **Journal of Geotechnical and Geoenvironmental Engineering**, **134(2)**. 175–184.

Borghei, M. S., Kabiri-Samani, A., and Banihashem, S. A. (2012). Influence of unsteady flow hydrograph shape on local scouring around bridge pier. **Proceedings of the Institution of Civil Engineers-Water Management**, **165(9)**. 473–480.

Breusers, H. N. C., Nicollet, G., and Shen, H. W. (1977). Local Scour Around Cylindrical Piers. **Journal of Hydraulic**, **15(3)**. 211–252.

Briaud, J. L., Brandimarte, L., Wang, J., and D'Odorico, P. (2007). Probability of scour depth exceedance owing to hydrologic uncertainty. **Georisk**, **1(2)**. 77–88.

Briaud, J.-L., Chen, C.H., Kwak, K., Wang, J. and Xu, J. (2004). **The SRICOSEFA computer program for Bridge Scour. Invited Lecture.** Proceedings of the Second International Conference on Scour and Erosion, Singapore (World Scientific Publishing Company: Singapore). 348-360.

Chilean Ministry of Public Works (MOP) (2020). **Highways Design Manual (In Spanish)**. Santiago, Chile.

Chilean National Water Agency (DGA) (2021). **Streamflow gauges (SFG)**. Available from: <https://dga.mop.gob.cl/servicioshidrometeorologicos/Paginas/default.aspx> [Accessed March 2020].

Chilean Railway Company (EFE) (2020). **Diagnosis of infrastructure of bridges and embankments of the EFE railway network (in Spanish)**.

Chow, V.T. (1994). **Hidráulica de canales abiertos**. Bogotá: Mc Graw Hill.

Cook, W., Barr, P. J., and Halling, M. W. (2015). Bridge Failure Rate. **Journal of Performance of Constructed Facilities**, **29(3)**. 04014080.

Cunnane, C. (1973). A particular comparison of annual maxima and partial duration series methods of flood frequency prediction. **Journal of Hydrology**, **18(10)**. 257–271.

Dargahi, B (1990). Controlling Mechanism of Local Scouring. **Journal of Hydraulic Engineering**, **116(10)**. 1197–1214.

Dey, S. (1999). Time-variation of scour in the vicinity of circular piers. **Proceedings of the Institution of Civil Engineers - Water, Maritime and Energy**, **136(2)**. 67–75.

German Association for Water, Wastewater and Waste (DWA) (2020). **Merkblatt DWA-M 529: Auskolkungen an pfahlartigen Bauwerksgründungen**. ISBN 978-3-96862-066-4.

Hong, J. H., Guo, W. D., Chiew, Y. M., and Chen, C. H. (2016). A new practical method to simulate flood-induced bridge pier scour-A case study of Mingchu bridge piers on the Cho-Shui River. **Water (Switzerland)**, **8(6)**. 23.

Jain, S. C., & Fischer, E. E. (1979). Scour around circular bridge piers at high Froude numbers. **No. FHWA-RD-79-104 Final Rpt.** 70.

Jain, S. C., & Fischer, E. E. (1980). Scour around bridge piers at high flow velocities. **Journal of the Hydraulics Division**, **106(11)**. 1827–1842.

Johnson, P.A., and Ayyub, B.M. (1992). Assessing time variant bridge reliability due to pier scour. **Journal of Hydraulic Engineering**, **118(6)**. 887–903.

Johnson, P. A., and Dock, D. A. (1998). Probabilistic bridge scour estimates. **Journal of Hydraulic Engineering**, **124**(7). 750–754.

Lang, M., Ouarda, T.B.M.J., and Bobée, B. (1999). Towards operational guidelines for over-threshold modelling. **Journal of Hydrology**, **225** (3–4). 103–117.

Link, O., Castillo, C., Pizarro, A., Rojas, A., Ettmer, B., Escauriaza, C., and Manfreda, S. (2017). A model of bridge pier scour during flood waves. **Journal of Hydraulic Research**, **55**(3). 310–323.

Link, O., García, M., Pizarro, A., Alcayaga, H., and Palma, S. (2020). Local Scour and Sediment Deposition at Bridge Piers during Floods. **Journal of Hydraulic Engineering**, **146**(3). 04020003

López, G., Teixeira, L., Ortega-Sánchez, M., and Simarro, G. (2014). Estimating Final Scour Depth under Clear-Water Flood Waves. **Journal of Hydraulic Engineering**, **140**(3). 328–332.

Lu, J.-Y., Hong, J.-H., Su, C.-C., Wang, C.-Y., and Lai, J.-S. (2008). Field Measurements and Simulation of Bridge Scour Depth Variations during Floods. **Journal of Hydraulic Engineering**, **134**(6). 810–821.

Manfreda, S., Link, O., and Pizarro, A. (2018). A theoretically derived probability distribution of scour. **Water (Switzerland)**, **10**(11). 13.

Melville, B. W., and Coleman, S. E. (2000). Bridge Scour, **Water Resources Publications**: Littleton, CO, USA; ISBN 1887201181. 550.

Meyer-Peter, E., and Müller, R. (1948). **Formulas for bed-load transport**. Delft, Netherlands: International Association for Hydro-Environment Engineering and Research. Vol. A2 of Proc., 2nd IAHR Congress, 26.

Pizarro, A., Ettmer, B., Manfreda, S., Rojas, A. and Link, O. (2017). Dimensionless Effective Flow Work for Estimation of Pier Scour Caused by Flood Waves. **Journal of Hydraulic Engineering**, **143**(7). 06017006.

Qi, M., Li, J., and Chen, Q. (2016). Comparison of existing equations for local scour at bridge piers: Parameter influence and validation. **Nat. Hazards**, **82** (3). 2089–2105.

- Raudkivi, A.J. (1986). Functional trends of scour at bridge pier. **Journal of Hydraulic Engineering**, **1(1)**. 13.
- Shahriar, A. R., Montoya, B. M., Ortiz, A. C., and Gabr, M. A. (2021). Quantifying probability of deceedance estimates of clear water local scour around bridge piers. **Journal of Hydrology**, **597**. 126177.
- Sheppard, D. M., Melville, B., and Demir, H. (2014). Evaluation of Existing Equations for Local Scour at Bridge Piers. **Journal of Hydraulic Engineering**, **140(1)**. 14–23.
- Tubaldi, E., Macorini, L., Izzuddin, B. A., Manes, C., and Laio, F. (2017). A framework for probabilistic assessment of clear-water scour around bridge piers. **Structural Safety**, **69**. 11–22.
- Wardhana, K. & Hadipriono, F. C. (2003). Study of Recent Building Failures in the United States. **Journal of Performance of Constructed Facilities**, **17(3)**. 151–158.
- Zadeh, K. F., Nossent, J., Woldegiorgis, T. B., Bauwens, W., and van Griensven, A. (2019). Impact of measurement error and limited data frequency on parameter estimation and uncertainty quantification. **Environmental Modelling and Software**, **118(3)**. 35–47.
- Zanke, U. (1977). Neuer Ansatz zur Berechnung des Transportbeginns von Sedimenten unter Stromungseinfluss in German. Hannover, Germany: Mitteilungen des Franzius-Institut, **Technical Univ. Hannover**. **46**. 157–178.
- Zanke, U. (1982). Kolke am Pfeiler in richtungskonstanter Strömung und unter Welleneinfluß. Mitteilungen des Franzius-Instituts. **Technical Univ. Hannover**. **54**. 381–416.

Appendix 4.1 GRAPHIC ANALYSIS

In this section, graphics with the probability density, histogram, cumulative distribution and P-P plots are presented in Figures A.4.1 to A.4.4.



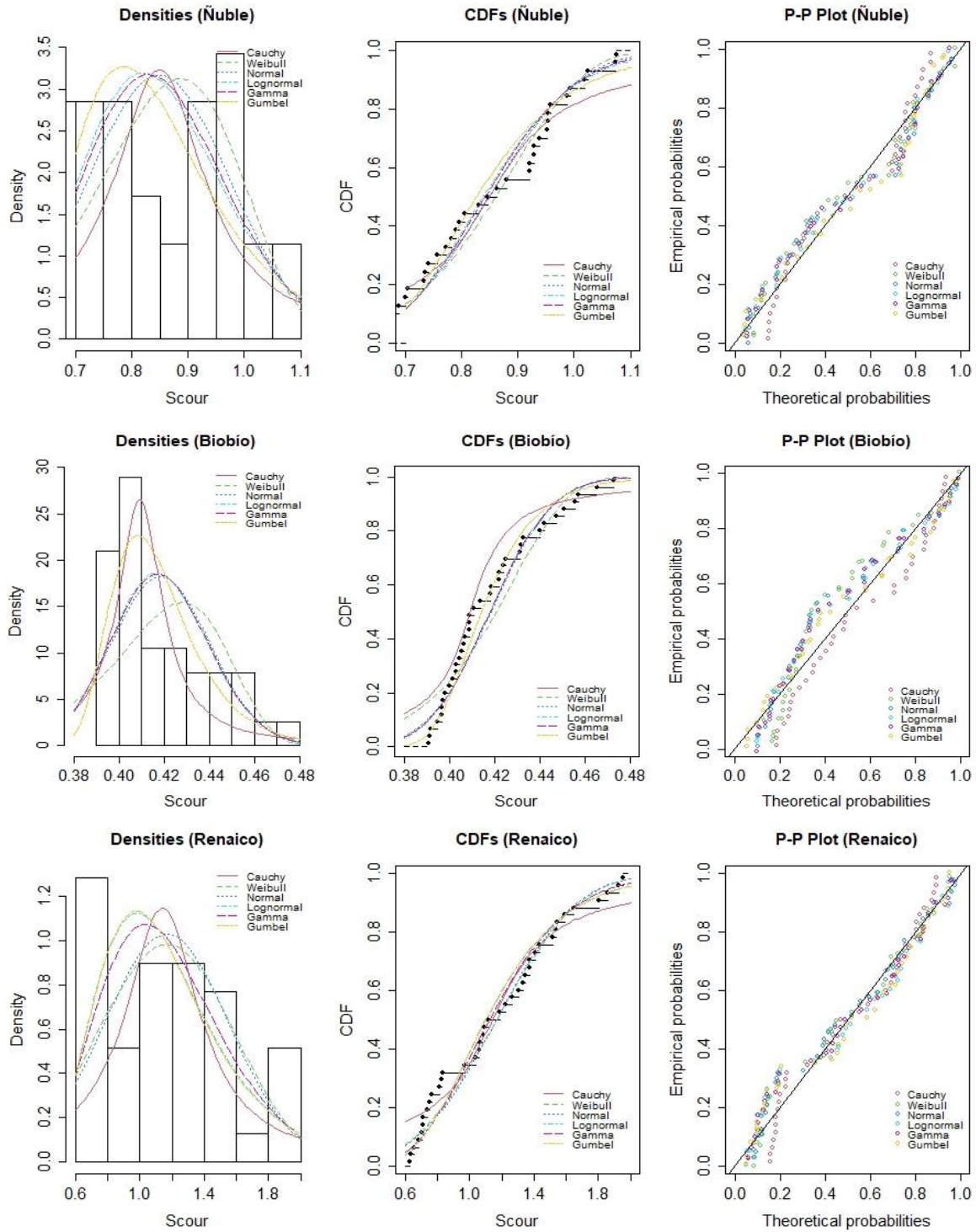


Figure A.4.1: Histogram and Density Function, Cumulative Density Function and P-P Plot of the local scour for Ñuble, Biobío and Renaico.

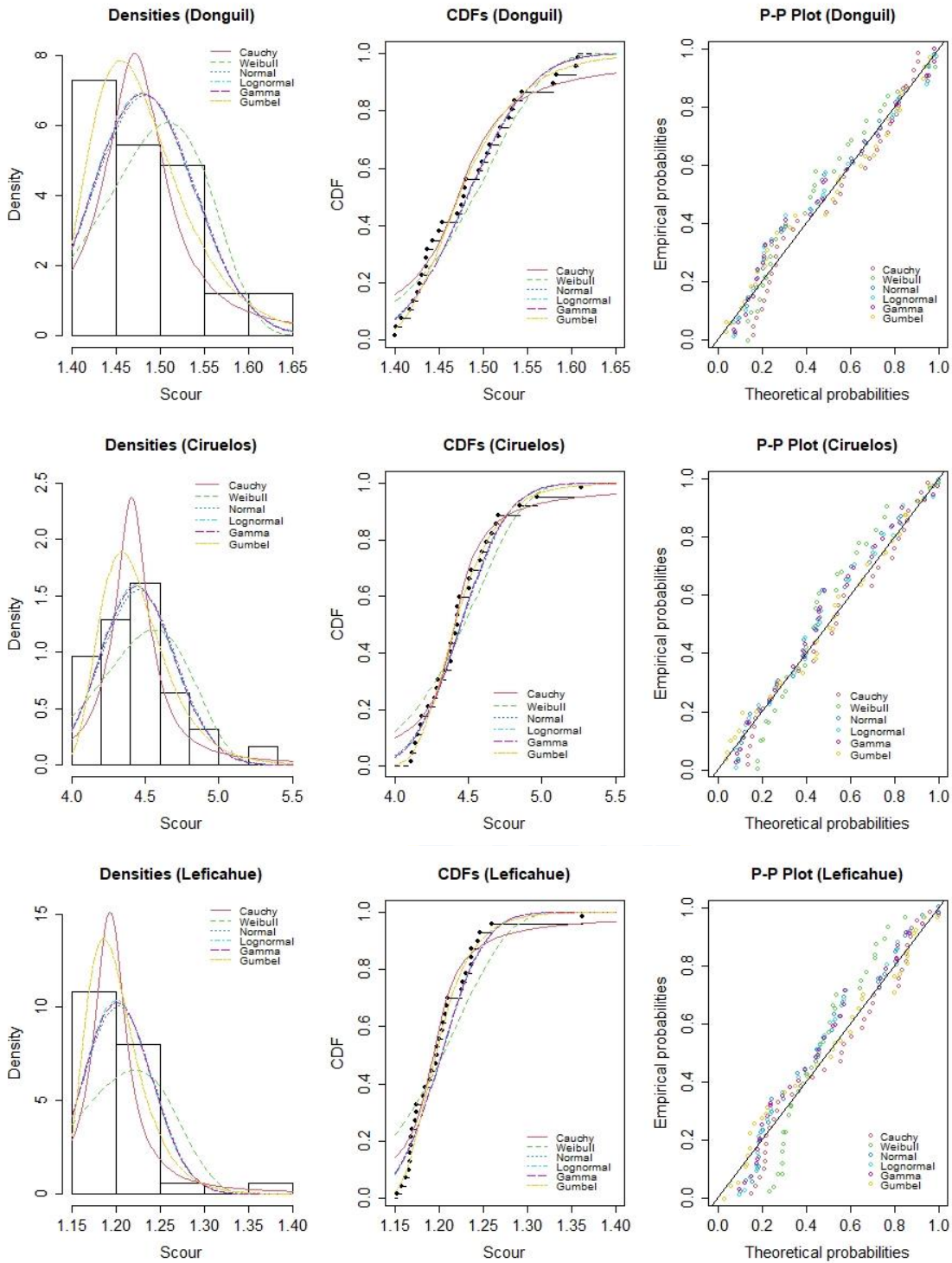


Figure A.4.2: Histogram and Density Function, Cumulative Density Function and P-P Plot of the local scour for Donguil, Ciruelos and Leficahue.

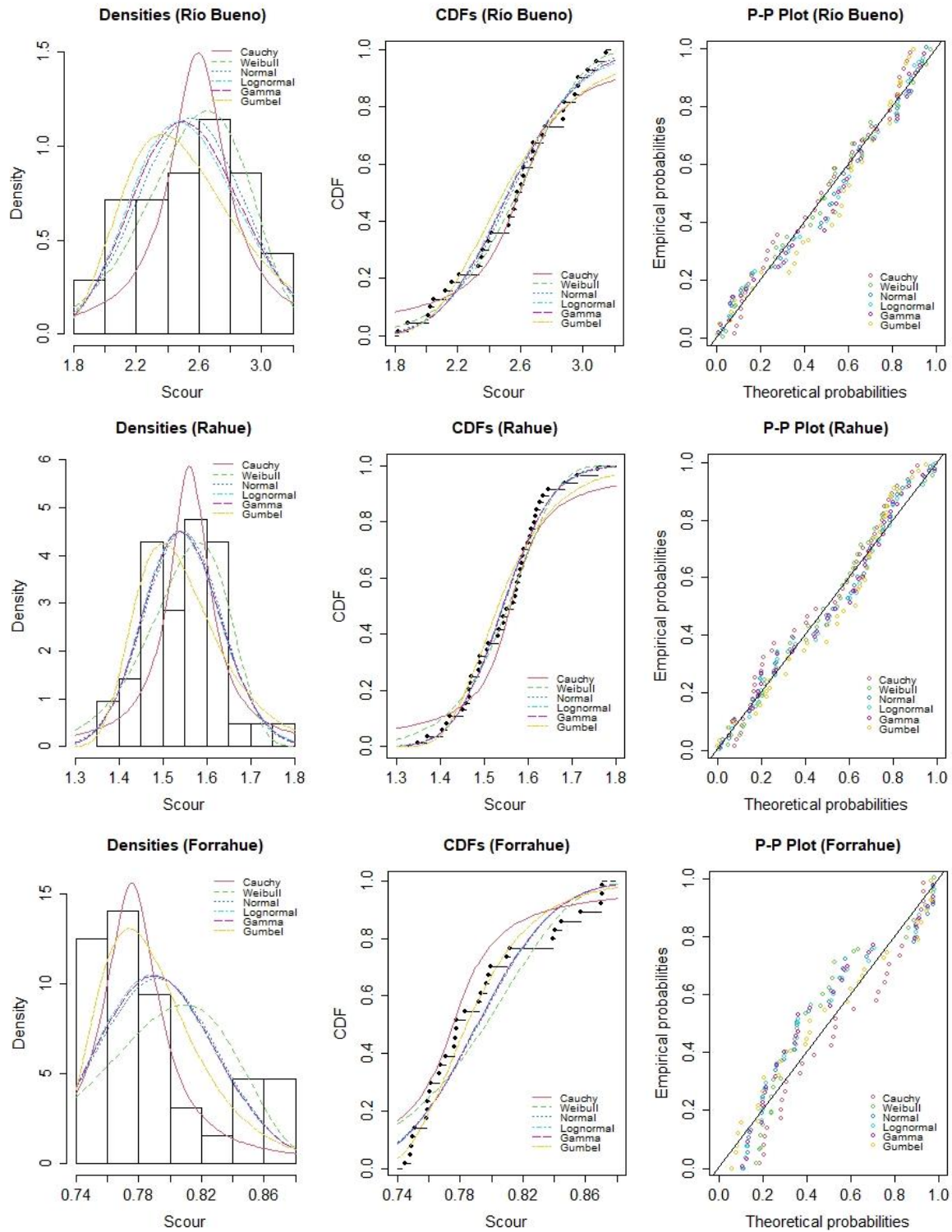


Figure A.4.3: Histogram and Density Function, Cumulative Density Function and P-P Plot of the local scour for Río Bueno, Rahue and Forrahue.

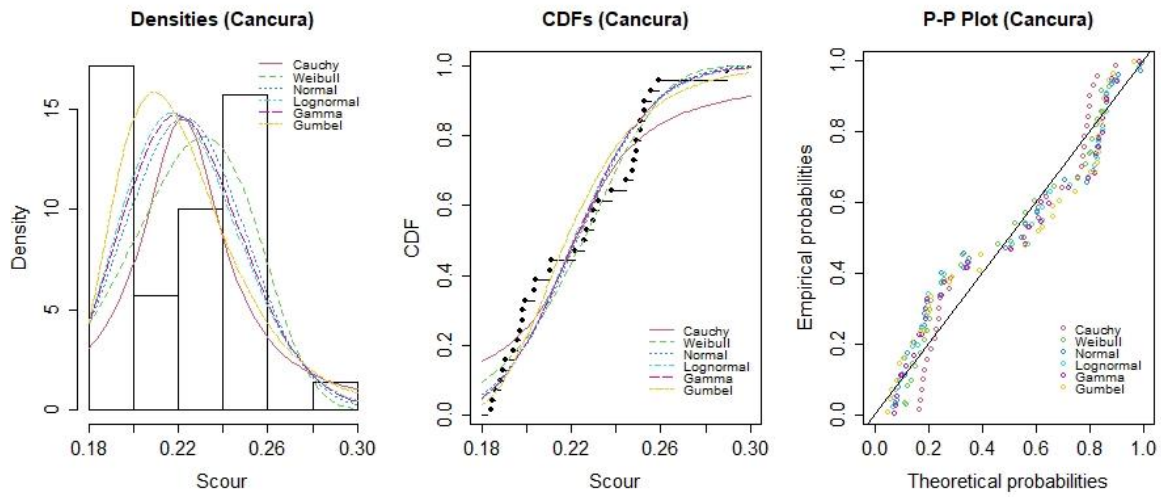


Figure A.4.4: Histogram and Density Function, Cumulative Density Function and P-P Plot of the local scour for Cancura.

